BOULDER 1, STATION 2, APOLLO 17: PETROLOGY AND PETROGENESIS

GRAHAM RYDER, DOUGLAS B. STOESER,* URSULA B. MARVIN, JANICE F. BOWER, and JOHN A. WOOD

Center for Astrophysics, Cambridge, Mass., U.S.A.

(Received 31 August, 1975)

Abstract. Boulder 1, Station 2, Apollo 17 is a stratified boulder containing dark clasts and dark-rimmed light clasts set in a light-gray friable matrix. The gray to black clasts (GCBx and BCBx) are multigenerational, competent, high-grade metamorphic, and partially melted breccias. They contain a diverse suite of lithic clasts which are mainly ANT varieties, but include granites, basaltic-textured olivine basalts, troctolitic and spinel troctolitic basalts, and unusual lithologies such as KREEP norite, ilmenite (KREEP) microgabbro, and the Civet Cat norite, which is believed to be a plutonic differentiate. The GCBxs and BCBxs are variable in composition, averaging a moderately KREEPy olivine norite. The matrix consists of mineral fragments derived from the observed lithologies plus variable amounts of a component, unobserved as a clast-type, that approximates a KREEP basalt in composition, as well as mineral fragments of unknown derivation. The high-temperature GCBxs cooled substantially before their incorporation into the friable matrix of Boulder 1.

The light friable matrix (LFBx) is texturally distinct from the competent breccia clasts and, apart from the abundant ANT clasts, contains clasts of a KREEPy basalt that is not observed in the competent breccias. The LFBx lacks such lithologies as the granites and the Civet Cat norite observed in the competent breccias and in detail is a distinct chemical as well as textural entity. We interpret the LFBx matrix as Serenitatis ejecta deposited in the South Massif, and the GCBx clasts as remnants of an ejecta blanket produced by an earlier impact. The source terrain for the Serenitatis impact consisted of the competent breccias, crustal ANT lithologies, and the KREEPy basalts, attesting to substantial lunar activity prior to the impact. The age of the older breccias suggests that the Serenitatis event is younger than 4.01 ± 0.03 b.y.

1. Introduction

Boulder 1, Station 2 is a layered, foliated, light-gray breccia that may represent the blue-gray unit exposed at the top of the South Massif (AFGIT, 1973). It was the only boulder of its kind observed by the astronauts, and four samples, believed to represent three clasts and the matrix, were collected from it. Macroscopic studies on the lunar surface (Schmitt, 1973) and in the laboratory (Marvin, 1974, 1975) showed that the boulder consisted of a variety of dark and light lithic clasts set in a lighter-gray friable matrix; some of the clasts were rimmed with dark aphanitic materials. The matrix materials and some of the larger clasts were singled out for consortium study, while smaller clasts were studied only petrographically as they were discovered in thin sections.

We have investigated clasts and matrices using petrographic and microprobe methods in an attempt to define the characteristics and history of the boulder and to extrapolate to an understanding of the nature of the lunar crust prior to the formation

* Current address U.S. Geological Survey, c/o U.S. Embassy, APO N.Y. 09697, U.S.A.

The Moon **14** (1975) 327–357.

of the boulder. Analytical techniques are as in Wood *et al.* (1971). This paper summarizes our observations and attempts to interpret the boulder in the light of the consortium studies.

For perspective, Figure 1 is a generalized schematic of the relative history of the main boulder materials as we interpret it. The details are more complex and will be discussed in later sections, after the characteristics of the lithic clast-types, including pigeonite basalts, have been outlined.

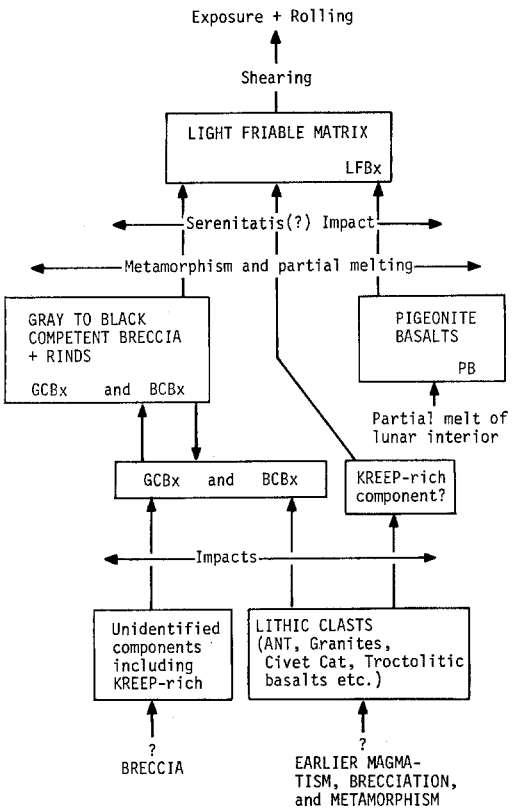

Fig. 1. Schematic simplified diagram for relative boulder history as inferred from thin section studies.

2. Clastic Materials

The four samples from different parts of the boulder include three samples of the large dark clasts (most of 72215 and 72255, and clast # 2 of 72275), and two samples of the boulder matrix (72275 and part of 72235) (Marvin, 1975). Table I outlines the main types of clastic materials observed in thin sections, and brief descriptions of these are presented below. Some of their major chemical characteristics are shown in Figures 2–4 and Table II. The data is from defocussed-beam analyses and compares favorably with analyses of similar materials by other methods (see Blanchard *et al.*,

TABLE I

Lithic clast-types and frequency of occurrence

(1) Basalt-textured rocks	
(a) Quartz-normative (KREEPy) pigeonite basalt (PB)	common
(b) Olivine-normative pigeonite basalt (OB)	scarce
(c) Mafic troctolitic basalt (TB)	scarce
(d) Pink spinel troctolitic basalt (PSTB)	scarce
(2) ANT suite	abundant
(3) Civet Cat norite (CN)	1 large fragment, few others
(4) KREEP norite	1 fragment
(5) Granites	frequent
(6) Ilmenite microgabbro	very rare
(7) Ultramafics	very rare
(8) Glassy clasts	very rare
(9) Devitrified maskelynite	frequent
(10) Monomineralic fragments	abundant
(11) Gray competent breccia (GCBx) to Black competent breccia (BCBx)	abundant

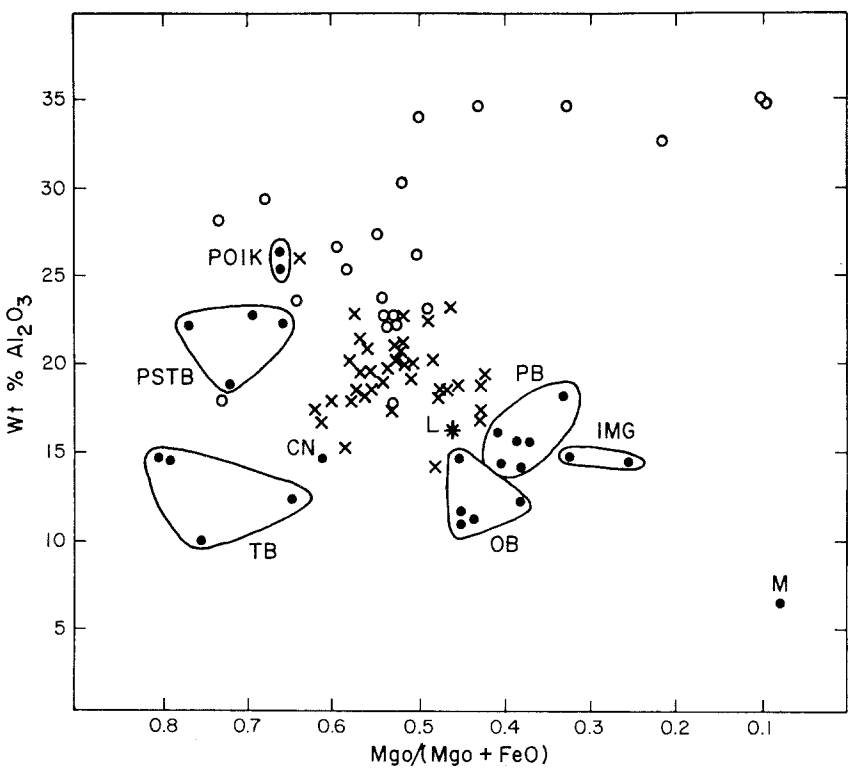

Fig. 2. Al_2O_3 v. MgO/(MgO+FeO) diagram for boulder lithologies. O=ANT; X=GCBx/BCBx; L*=LFBx; PB=KREEPy basalt; M=Mesostasis of KREEPy basalt; OB=Olivine-normative pigeonite basalt; TB=Mafic troctolitic basalt; PSTB=Pink spinel troctolitic basalt; CN=Civet Cat norite; POIK=Poikilitic ANT; IMG=Ilmenite microgabbro.

TABLE II

Representative DBA analyses of Boulder 1, Station 2 lithologies

	(1)	(2)	(3)	(4)	(5)	(6)	(7)	(8)	(9)
SiO_2	49.37	49.61	45.47	45.37	45.64	44.2	48.41	46.43	46.26
TiO_2	0.92	1.18	0.49	0.23	0.13	0.1	0.11	0.12	0.19
Al_2O_3	18.12	15.65	11.03	14.73	20.72	29.4	22.56	26.89	25.55
Cr_2O_3	0.36	0.33	0.59	0.88	0.09	0.1	0.07	0.07	0.10
FeO	8.45	11.26	16.97	12.75	5.05	3.7	7.08	3.47	4.15
MnO	0.17	0.18	0.27	0.26	0.06	tr.	0.08	0.06	0.10
MgO	4.23	6.98	13.17	10.58	17.69	7.8	8.17	6.97	7.76
CaO	12.57	10.90	10.22	11.45	12.46	15.9	13.46	15.15	14.40
Na_2O	0.56	0.60	0.16	0.13	0.40	0.2	0.64	0.44	0.38
K_2O	0.32	0.35	0.04	0.08	0.07	0.1	0.14	0.08	0.11
BaO	0.08	0.06	0.05	0.03	0.02	–	0.06	0.04	0.03
P_2O_5	0.53	0.58	0.01	0.02	0.02	tr.	0.60	0.01	–
Total	96.40	98.13	98.46	96.51	102.37	101.5	101.37	99.74	99.06
CIPW norm									
Fo	–	–	8.8	3.8	24.8	11.2	0.1	2.3	2.5
Fa	–	–	9.0	3.6	5.6	4.3	0.1	0.9	1.0
En	11.0	17.8	20.8	21.9	7.6	3.1	19.9	14.1	16.0
Fs	11.7	17.3	19.2	18.9	1.6	1.1	12.6	5.1	6.1
Wo	5.6	4.9	9.1	7.5	2.9	–	1.9	1.7	1.6
Or	2.0	2.1	0.2	0.5	0.4	0.6	0.8	0.5	0.7
Ab	4.9	5.2	1.3	1.1	3.3	1.9	5.4	3.7	3.2
An	47.9	39.8	29.7	40.8	53.3	77.5	57.5	71.4	68.3
Ilm	1.8	2.3	0.9	0.4	0.2	0.1	0.2	0.2	0.4
Cr	0.5	0.5	0.9	1.3	0.1	0.1	0.1	0.1	0.1
Qtz	11.3	7.5	–	–	–	–	–	–	–
Cor	–	–	–	–	–	0.1	–	–	–
Ap	1.3	1.3	–	–	–	–	1.3	–	–
MgO/MgO+FeO	0.334	0.383	0.437	0.453	0.778	0.678	0.536	0.667	0.651
No. of analyses (100 μ beam)	7	26	17	34	29	2×6	7	20	23

(1) Subophitic pigeonite basalt in 72275,136.
(2) Variolitic pigeonite basalt in 72275,128.
(3) Equigranular olivine-normative basalt in 72235,59.
(4) Subophitic olivine-normative basalt in 72235,59.
(5) Pink spinel troctolitic basalt in 72215,185.
(6) Granulitic ANT in 72275,128.
(7) Granulitic ANT in 72215,180.
(8)–(9) Poikilitic ANTs in 72215,180.

	(10)	(11)	(12)	(13)	(14)	(15)	(16)	(17)	(18)
SiO_2	48.48	45.89	49.05	48.02	45.1	47.7	47.0	46.71	53.17
TiO_2	6.59	4.38	0.98	0.66	0.6	1.1	1.0	2.05	0.92
Al_2O_3	14.54	14.70	18.73	18.79	20.0	20.3	22.8	20.11	12.27
Cr_2O_3	0.05	0.05	0.04	0.04	0.2	0.2	0.2	0.25	0.18
FeO	10.01	11.70	8.60	8.00	7.7	10.6	8.9	8.44	10.99
MnO	0.14	0.17	0.11	0.12	0.1	0.2	0.1	0.12	0.12
MgO	3.38	5.67	7.88	7.32	9.1	10.0	8.7	8.99	9.52
CaO	9.42	12.16	12.39	11.81	12.7	11.5	12.9	12.13	8.69
Na_2O	0.85	0.91	0.63	0.77	0.5	0.5	0.6	0.68	0.45
K_2O	0.90	0.92	0.91	1.02	0.2	0.2	0.2	0.35	1.94
BaO	0.11	0.11	0.15	0.09	–	–	–	0.02	–
P_2O_5	0.42	0.46	0.57	0.34	0.2	0.4	0.5	0.29	0.38
Total	95.05	97.27	100.05	97.00	99.9	102.7	102.9	100.17	98.63
CIPW norm									
Fo	–	–	–	–	–	3.4	4.5	1.8	–
Fa	–	–	–	–	–	2.7	3.3	1.1	–
En	8.9	14.5	19.7	18.8	20.7	19.5	14.8	15.8	24.1
Fs	7.7	14.6	14.4	14.2	15.2	13.9	9.9	10.7	18.6
Wo	4.8	10.3	5.1	5.0	1.0	0.7	0.8	3.2	6.3
Or	5.6	5.6	5.4	6.2	0.8	1.3	1.3	2.1	11.6
Ab	7.6	7.9	5.4	6.7	3.7	4.2	4.9	5.8	3.9
An	35.0	34.3	45.6	46.2	55.8	51.1	57.4	50.7	26.1
Ilm	13.2	8.6	1.9	1.3	1.2	2.0	1.8	3.9	1.8
Cr	0.1	0.1	0.1	0.1	0.1	0.3	0.3	0.4	0.3
Qtz	15.8	2.7	1.3	0.6	0.2	–	–	–	6.3
Cor	–	–	–	–	–	–	–	–	–
Ap	1.0	1.0	1.3	1.8	1.1	1.0	1.0	0.7	0.9
MgO/MgO+FeO	0.252	0.326	0.478	0.478	0.541	0.485	0.494	0.516	0.464
No. of analyses (100 μ beam)	4	12	16	15	26	21	15	18	24

(10)–(11) Ilmenite microgabbros in 72275,142.
(12) Domain 5 B/GCBx in 72215,178.
(13) Domain 5 B/GCBx in 72215,180.
(14) GCBx matrix of 72255,95.
(15) GCBX matrix of clast in 72275,134.
(16) GCBx matrix of clast in 72275,146.
(17) Vesicular GCBx clast in 72235,59.
(18) Partially molten matrix in 72215,180. Domain 5 (area in Figure 11d).

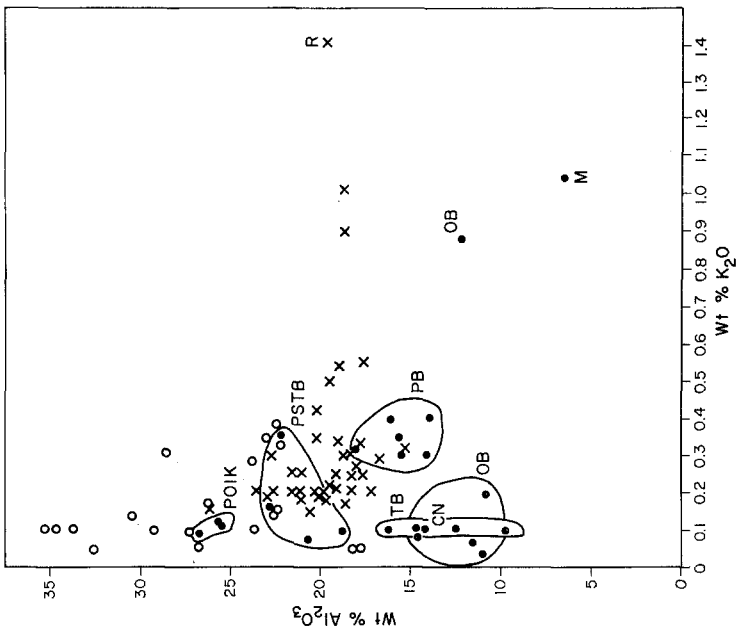

Fig. 4. Al_2O_3 v. K_2O diagram for boulder lithologies. Symbols and abbreviations as in Figure 2. R: Metamorphosed breccia rim on granite clast.

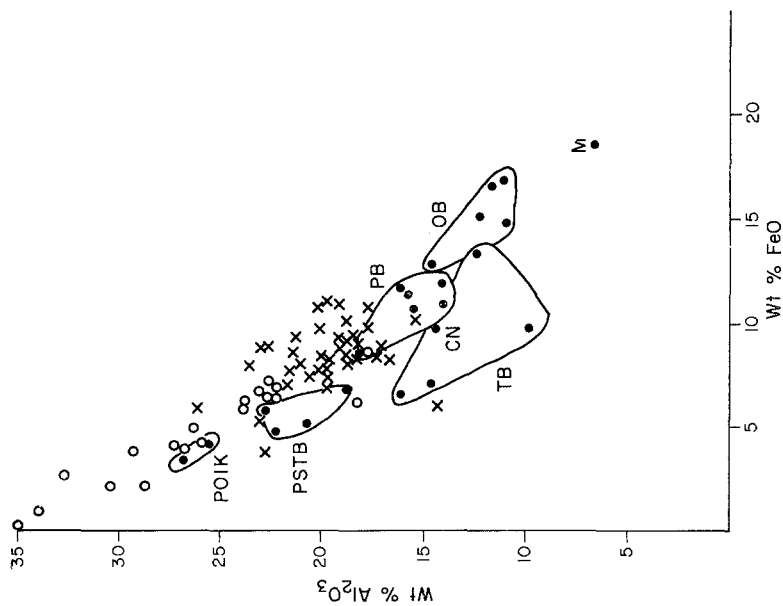

Fig. 3. Al_2O_3 v. FeO diagram for boulder lithologies. Symbols and abbreviations as in Figure 2.

1975). In Table I we have attempted to point out the relative abundances of the clast-types. Point counts have not been undertaken because we do not know exactly how representative our samples may be, and the precision gained would be of spurious accuracy, carrying little information. In addition to those listed, both the Marble Cake clast (from 72275) and the Dying Dog clast (sample 72235), examples of the rimmed complex clasts, are also briefly described.

Although lithic clast sizes range down to less than 100 μ, the petrographic studies were concentrated on those fragments larger than 200 μ. The gray to black competent breccias (GBCx and BCBx respectively) must be distinguished from other lithic clast-types because, with one exception, all the other clast-types are found within them.

More detailed reports on the petrography and microprobe studies may be found in Stoeser *et al.* (1974a, b, c).

2.1.1. *Quartz-Normative (KREEPy) Pigeonite Basalt (PB)*

Zones of basaltic clasts were macroscopically recognized in the 72275 light-gray matrix (Marvin, 1975), and are referred to elsewhere in the Consortium Indomitabile literature as pigeonite basalts (PB). Thin sections reveal that they are non-mare basalts, present as individual clasts and as clots and lenses of breccia composed almost entirely of basalt. The petrography of these clasts has been briefly reported by Stoeser *et al.* (1974a, b, c). Most of the clasts have subophitic to intersertal textures (Figure 5a), but finer-grained variolitic and equigranular types are also found. The basalts are moderately KREEPy (Table II, cols. 1–2 and Blanchard *et al.* (1975)), and are fractionated ($MgO/MgO+FeO \sim 0.3$–0.4). They contain equal proportions of plagioclase ($An_{94}Or_1$ zoned to $An_{76}Or_8$; Figure 6) and pyroxene (mainly pigeonite, Figure 7) with 10–20% of an opaque mesostasis. Only one olivine crystal ($\sim Fo_{70}$) has been observed, while a silica mineral (cristobalite?) is commonly present as an interstitial phase, sometimes up to 500 μ long. The mesostasis is iron-rich and mineralogically complex, containing ferroaugite, ilmenite, Fe-metal, troilite, silica, barian K-feldspar, plagioclase, a phosphate, and at least one Zr-mineral.

The low siderophile contents (Morgan *et al.*, 1975), the basaltic textures with a lack of relict material, and the low nickel contents of the Fe-metal grains (unpublished analyses) suggest that this basalt-type is a partial melt of the lunar interior that was extruded onto the surface, rather than an impact melt of upper crustal material. The extrusion took place at about 4.01 b.y. (Compston *et al.*, 1975). PB clasts have been observed only in the light-gray friable matrix, and not within the GCBx or BCBx clasts.

2.1.2. *Olivine-Normative Pigeonite Basalts (OB)*

Small fragments (<3 mm) of this quantitatively minor group have only been definitely recognized in thin sections from 72215 and 72235, but may also be present in 72275 (Stoeser *et al.*, 1974a). The textures of these nonmare basalts range from porphyritic (Figure 5b) to subophitic (Figure 5c). Plagioclase (Figure 6), pigeonite (Figure 7), olivine (Figure 8), and chromite are present. Representative bulk defocussed-beam

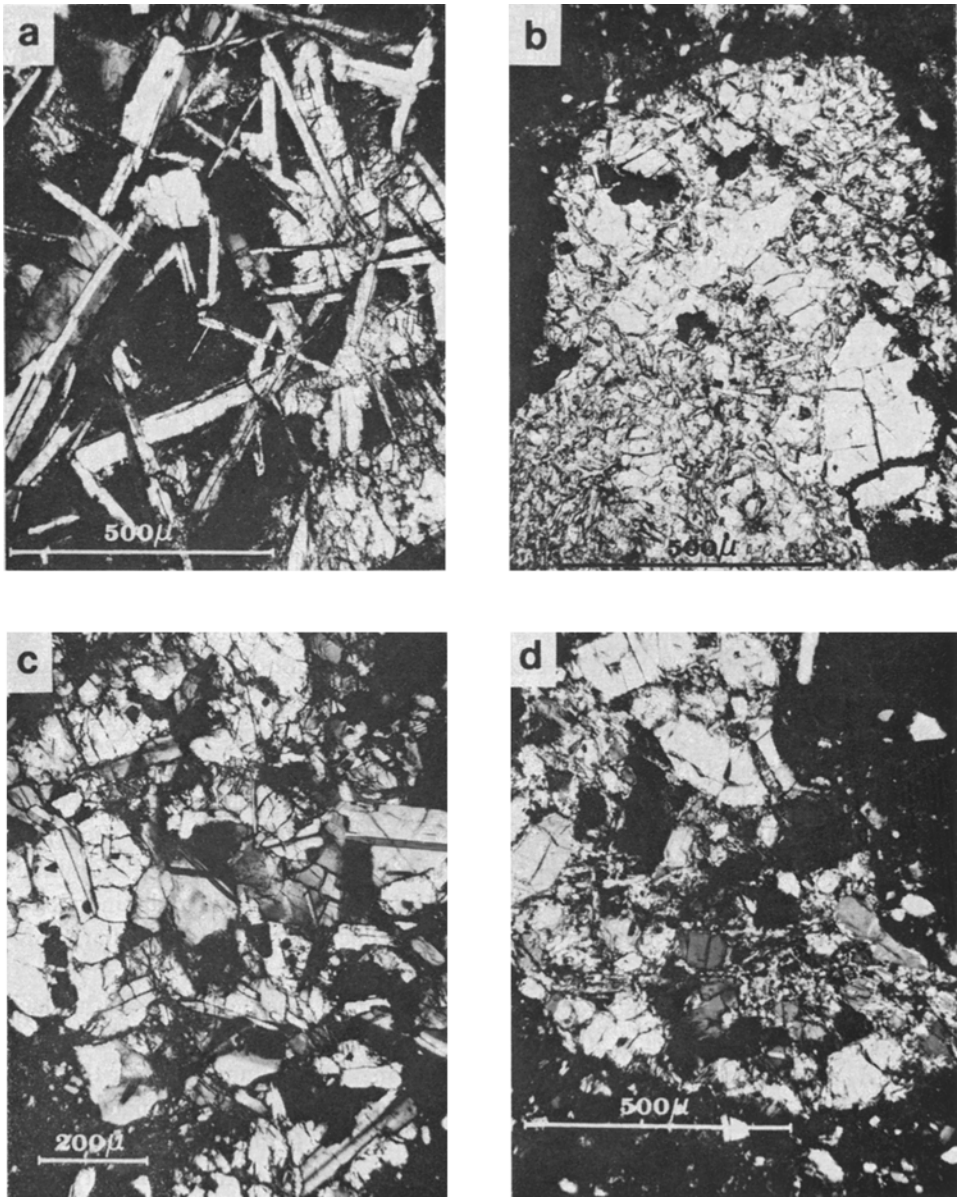

Fig. 5a–d.

Fig. 5. Photomicrographs of boulder lithologies: (a) subophitic-intersertal KREEPy basalt (PB), crossed polarisers; (b) porphyritic olivine-normative basalt (OB), crossed polarisers; (c) subophitic olivine-normative basalt (OB), crossed polarisers; (d) mafic troctolitic basalt (TB), crossed polarisers; (e) pink spinel troctolitic basalt (PSTB), crossed polarisers; (f) pink spinel troctolitic basalt (PSTB), reflected light. (S = spinel, O = olivine, Px = pyroxene, P = plagioclase.)

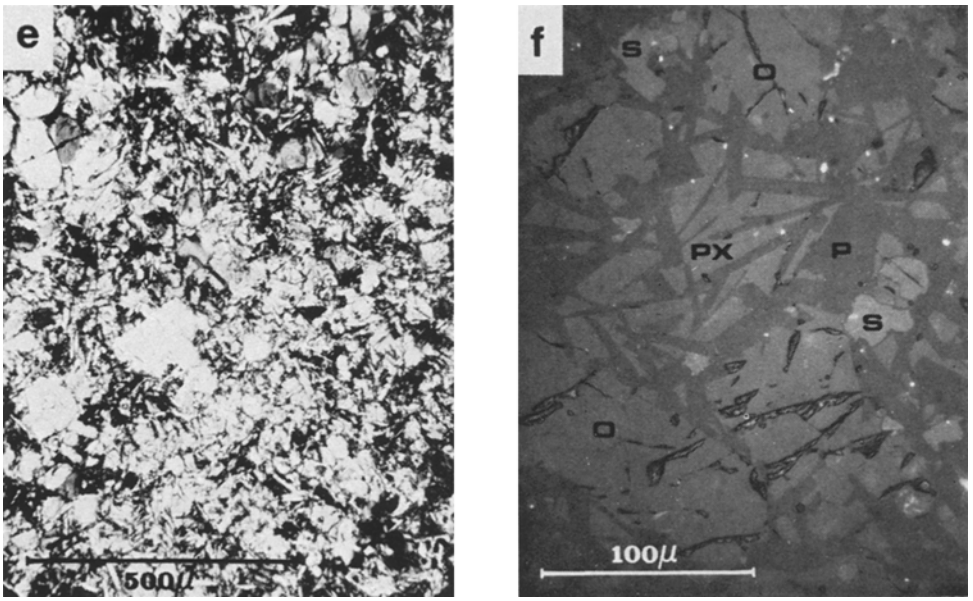

Fig. 5e–f.

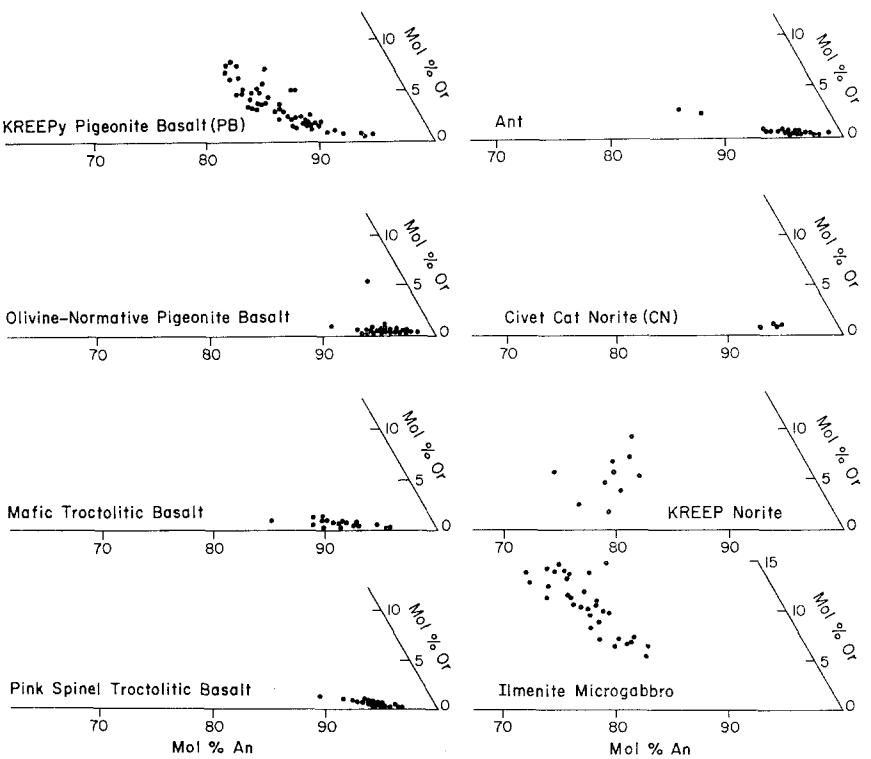

Fig. 6. Plagioclase compositions for boulder clasts on partial feldspar ternary diagram.

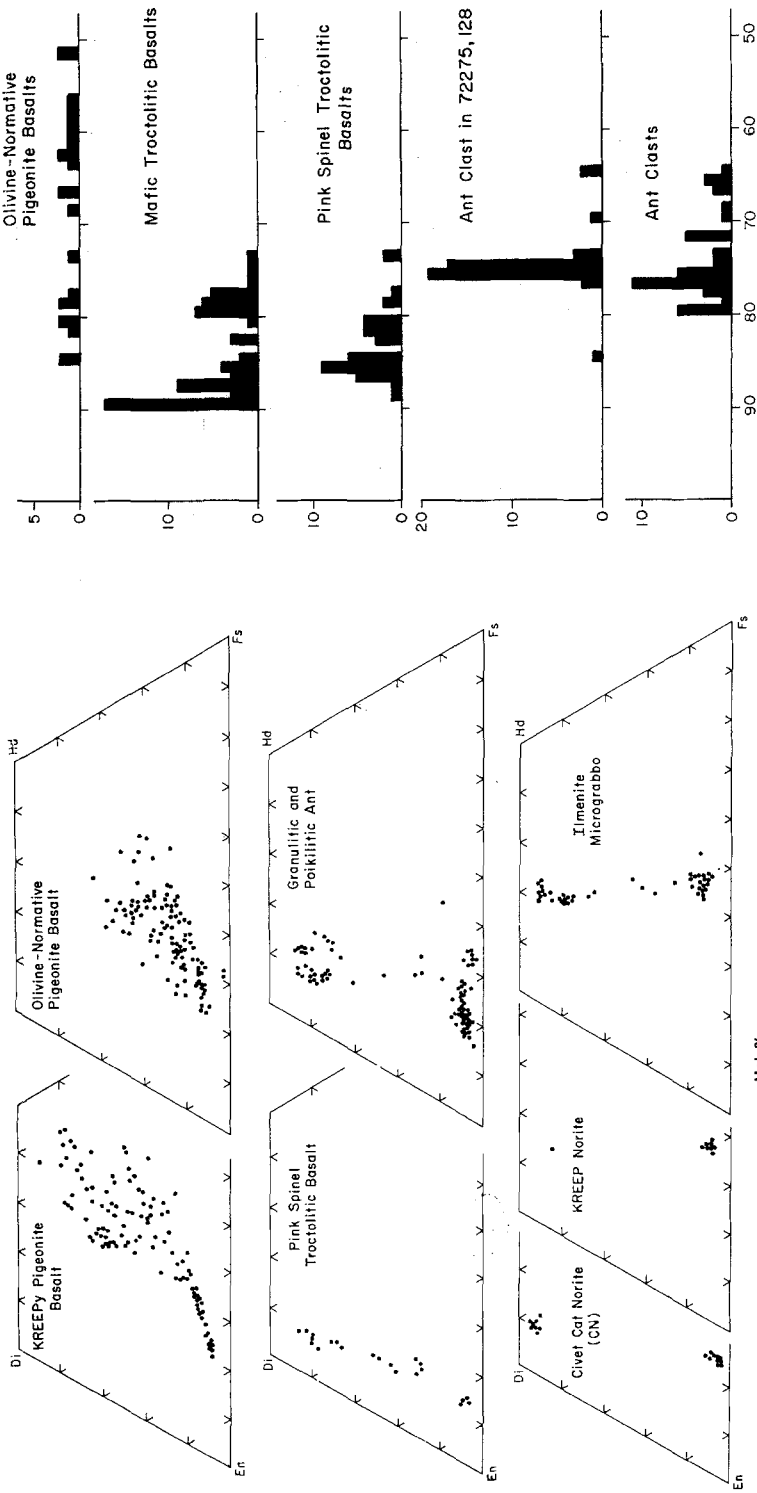

Fig. 8. Olivine composition histograms for boulder clasts.

Fig. 7. Pyroxene compositions for boulder clasts on pyroxene quadrilateral.

analyses are given in Table II (cols. 3–4); they are low in KREEP components. They differ from the PBs not only in their more anorthitic plagioclase and in their abundance of olivine, but also in their abundance of chromite and their lack of any obvious mesostasis. They are also chemically distinct from and not gradational to the PBs, and their textures (e.g. vitrophyric) are incompatible with a cumulate origin from PB magmas. They are a separate series, although they are similarly rather fractionated ($MgO/MgO+FeO \sim 0.35$–0.45).

2.1.3. *Mafic Troctolitic Basalts (TB)*

Subpoikilitic troctolitic or allivalitic basalts (Figure 5d) are disseminated throughout the boulder. They contain euhedral olivines about 200 μ in diameter set in a groundmass of plagioclase and rare Ca-poor pyroxene (?). They are more magnesian than the olivine-normative pigeonite basalts, a characteristic reflected in olivine compositions (Figure 8) that are more magnesian than most of the olivine compositions found in the anorthositic norites and troctolites of the boulder (Figure 8) and in, for example, the Luna 20 ANT suite (Prinz *et al.*, 1973; Taylor *et al.*, 1973). Many of the group are cataclasized, though the similarity of the original textures to the non-cataclasized varieties is usually apparent. This group may be gradational to the pink spinel troctolitic basalt group, but the latter are distinctly more aluminous (Figure 2).

2.1.4. *Pink Spinel Troctolitic Basalt (PSTB)*

All four boulder samples contain fragments of basaltic-textured spinel-bearing rocks. In most, olivine is phenocrystal (Figure 8); in some it appears only interstitially to the plagioclase laths. Ca-Mg-pyroxene (Figure 7) is a common interstitial phase. The largest fragment, 3 mm in diameter, contains 200-μ olivine phenocrysts set in a fine-grained matrix of plagioclase and interstitial pyroxene, olivine, and spinel (Figures 5e, 5f); only rarely are a silica mineral and a Si–K glassy mesostasis present. The spinel occurs in a reaction relationship, with embayed and irregular forms, and was a liquidus phase with the phenocrystal olivine. The olivines in the fragment have a narrow compositional range (Fo_{84-88}) similar to those of the Luna 20 spinel troctolites (Prinz *et al.*, 1973); the phenocrysts are slightly more magnesian than the groundmass olivine. The bulk composition of the fragment (Table II, col. 5) plots close to the olivine-spinel boundary curve in the An–Fo–si System for $Fe/Fe+Mg \sim 0.3$ (Walker *et al.*, 1973), consistent with the textural relationships. Spinel or olivine relicts from a possible source rock, as in 62295 (Walker *et al.*, 1973), have not been identified.

2.2. ANT SUITE, NORITES, AND TROCTOLITES

Texturally and chemically diverse plagioclase-rich lithic clasts are the most abundant clast-type in the boulder apart from the dark competent breccias, and are frequently rather large (several centimeters). They correspond loosely to the ANT suite chemically and mineralogically (Prinz *et al.*, 1973), though the compositions of some are more mafic than the formal definition of the suite allows. A few are also richer in *K* and *P* than any members of the ANT suite. Thus chemical relationships between members

of the group as we describe it may be tenuous or even non-existent. Many of the clasts appear to have originated as breccias, which have subsequently recrystallized. Our classification is based on texture and corresponds in part to the degree or style of thermal metamorphism experienced by the rocks.

2.2.1. *Unrecrystallized ANT Breccias*

This group consists of breccias with porous fragmental matrices and seems to have been derived from the crushing of crystalline anorthositic rocks. The crushing of some clasts was contemporaneous with the deformation of the enclosing breccia matrix in which they are found as clots; other brecciation pre-dates the deformation.

2.2.2. *Granulitic ANT*

Abundant fragments are characterized by the textures and triple points typical of subsolidus recrystallization (Figure 9a); some are equigranular, while others are seriate. The compositions are very variable (Table II, cols. 6–7), ranging from anorthositic to noritic and troctolitic; some of the anorthositic varieties are probably recrystallized single mineral fragments derived from coarse noritic rocks (e.g. Wilshire and Jackson, 1972). Troctolitic varieties are about as abundant as noritic varieties. Many are clearly recrystallized breccias with larger clasts of plagioclase, olivine, and pyroxene seated in a recrystallized granulitic matrix (Figure 9b); the equigranular varieties have a more equivocal origin. The compositional ranges for plagioclase (Figure 6), pyroxene (Figure 7), and olivine (Figure 8) fall in the compositional fields established for other ANT samples (Prinz *et al.*, 1973; Taylor *et al.*, 1973). Within a given clast, the compositional fields are rather narrow (e.g. olivine, Figure 8).

2.2.3. *Poikilitic ANT*

This distinct group is common in 72215 but sparse elsewhere. The mineralogy is similar to other ANT textural types. The coarse poikilitic texture (Figure 9c) consists of equidimensional chadacrysts of plagioclase (An_{90-96}) seated in pyroxene oikocrysts (En_{74-77} Wo_{3-5}); augite and olivine are also present, though minor. The oikocrysts have maximum diameters larger than 4 mm. The two clasts of this rock-type which have been analyzed (Table II, cols. 8–9) are anorthositic norites, compositionally similar to many granulitic ANT clasts. Small spherical inclusions of olivine and pyroxene (?) in some of the plagioclases suggest that these may be high-grade metamorphic rocks, but the overall texture is more ambiguous than in the poikiloblastic ANT group (below), and they could be melt-rocks.

2.2.4. *Poikiloblastic ANT*

Fine-grained ($< 200\ \mu$) rocks, consisting of poikilitic pyroxenes enclosing small stubby euhedral plagioclases ($< 20\ \mu$) set in a mosaic of coarser anhedral plagioclases (Figure 9d), are found in 72215 and 72235, and more rarely in the other boulder samples. Occasional poikiloblastic patches in the granulitic ANT fragments suggest that the poikiloblastic texture is an advanced stage of the granulitic recrystallization.

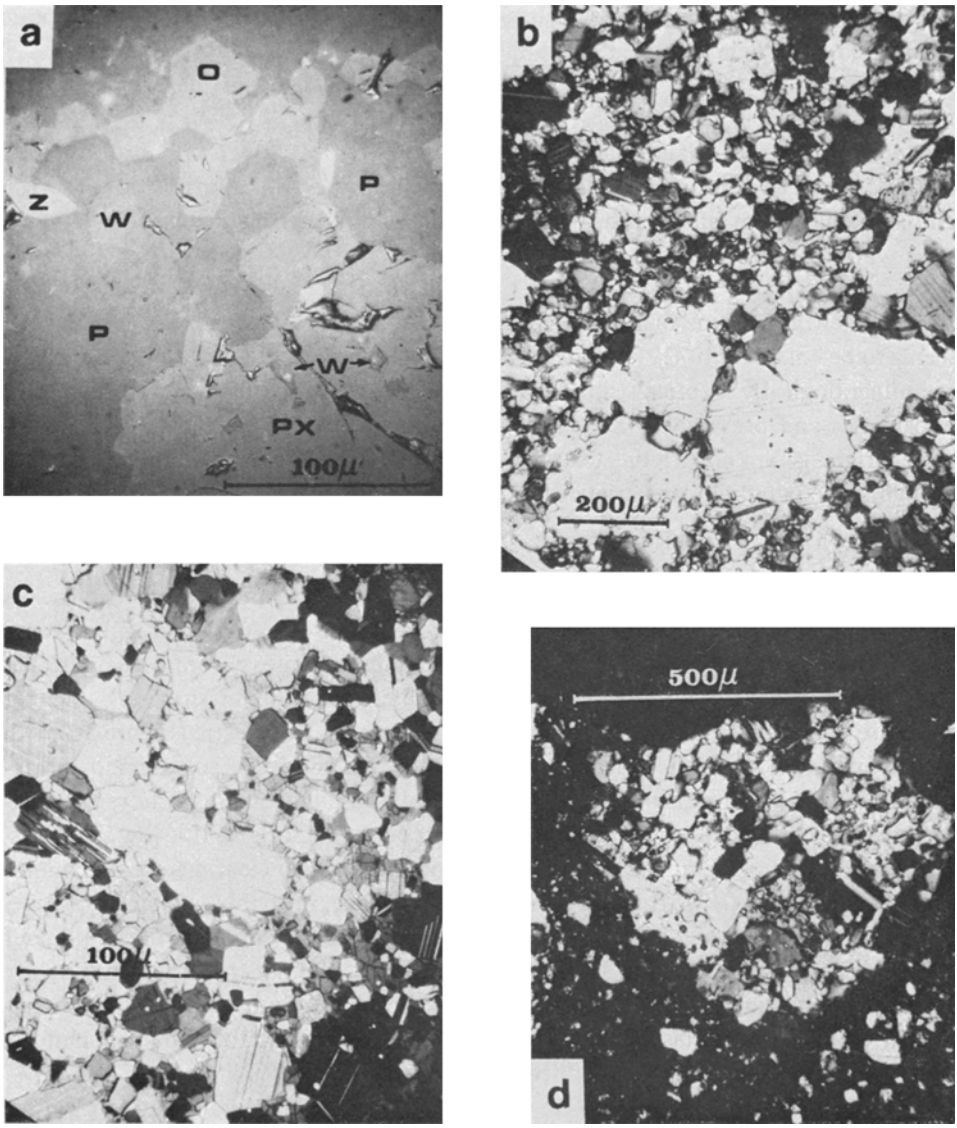

Fig. 9. Photomicrographs of ANT lithologies: (a) Granulitic ANT variety showing recrystallized texture. O=olivine, P=plagioclase, Px=orthopyroxene, W=phosphate phase, Z=zircon. Reflected light. (b) Granulitic ANT, recrystallized breccia. Crossed polarisers. (c) Poikilitic ANT with large continuous orthopyroxene enclosing stubby plagioclases. Crossed polarisers. (d) Poikiloblastic ANT, recrystallized breccia, with poikilitic patches. Crossed polarisers.

The textures of the poikiloblastic clasts do not closely resemble those of the Apollo 16 POIK rocks (Bence *et al.*, 1973; Simonds *et al.*, 1973).

2.2.5. *Coarse ANT*

Some clasts are too small, relative to their grain size, to allow a definition of their textures. Some appear to be coarse cataclastic anorthosites and anorthositic 'gabbros', and some have been shocked heavily enough to vitrify their plagioclases.

2.2.6. *K-ANT*

A special chemical type of brecciated and granulitic ANT is *K*- and/or *P*-rich, and seems to be confined to 72215. A detailed study has not been made, but the fragments are mineralogically identical to the other ANT fragments except for the presence of phosphates and presumably *K*-rich plagioclase, and possibly *K*-feldspar. Their ultimate origin is unknown; the textures are mainly those of recrystallized breccias, though some equigranular varieties are more equivocal.

2.3. Civet cat norite (CN)

The 2.5-mm Civet Cat clast in 72255 was selected for consortium study. The rock is essentially bimineralic, consisting of orthopyroxene ($En_{72-75}Wo_{2-4}$, Figure 7) and plagioclase (An_{92-94}, Figure 6). Augite, cristobalite, ilmenite, chromite, troilite, Fe-metal, baddeleyite, zircon, Zr-bearing armalcolite, and niobian rutile (?) together comprise less than 1% of the rock. Though its texture is cataclastic (Figure 10) with kinked pyroxene, the relict primary texture, the wide pyroxene solvus, and the restricted mineral compositions suggest either a plutonic igneous or a thoroughly recrystallized rock; we favor an igneous, probably cumulate, origin. It is low in alkalis, REEs, and uranium (Blanchard *et al.*, 1975) and lacks any ancient meteoritic component (Morgan *et al.*, 1975); it has a Rb/Sr isochron age, probably igneous, of $4.17 \pm \pm 0.04$ b.y. (Compston *et al.*, 1975). It may be related to the cumulate norite boulder collected from the Sculptured Hills area at Station 8, though the latter has slightly more calcic plagioclase and magnesian pyroxene (McCallum *et al.*, 1975). Other smaller Civet Cat-type clasts and mineral fragments occur in all four boulder samples, but have not been positively identified within the LFBx.

2.4. KREEP norite

A 3-mm yellowish-brown clast embedded in a layer of light-colored gabbroic anorthosite was a conspicuous surface feature of 72235 (Stoeser *et al.*, 1974a). The clast consists of about equal proportions of plagioclase and pyroxene with 1% accessory minerals, mainly ilmenite and troilite, and traces of phosphate. Plagioclase (An_{71-79}, Figure 6) high in orthoclase components ($\sim Or_6$) is interlocked with pyroxene (En_{59-61} Wo_{3-6}, Figure 7) that has an internal polygonal texture (Figure 10b) indicative of incomplete recrystallization of large primary crystals. Mineralogically the clast is unlike any other described lunar rock-type and is not observed elsewhere in the boulder.

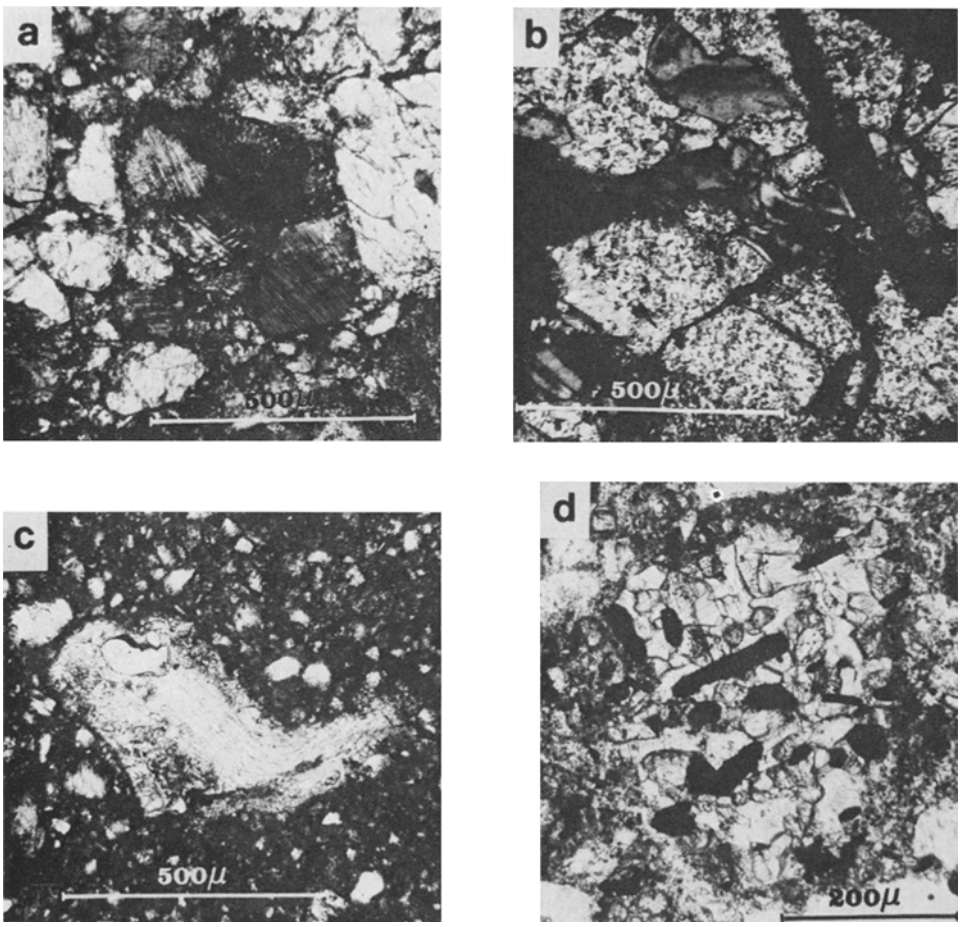

Fig. 10. Photomicrographs of boulder clast lithologies: (a) Civet Cat norite, showing cataclasized pyroxene and plagioclase. Crossed polarisers. (b) KREEP norite, showing granular pyroxene. Crossed polarisers. (c) Granite fragment, of deformed silica bars in a Si–K–rich glass. Fragment is embedded in GCBx. Plane polarised light. (d) Ilmenite microgabbro, with ilmenite (black) set in a granulitic plagioclase/pyroxene ground. Plane polarised light.

2.5. Granites

Small 'granite' clasts, usually less than 500 μ, are abundant within the GCBxs and BCBxs and are discussed in detail elsewhere (Ryder *et al.*, 1975). Texturally and chemically diverse, they probably represent the remnants of melting of an original granite source-rock; some clasts are completely glassy, while others are completely holocrystalline. Silica embedded in glass (Figure 10c) and silica feldspar intergrowths are the commonest varieties. At least some of the granites were liquid at the time of the aggregation of their host breccias. An unusual characteristic is the presence of Ca–K-feldspars, whose nature and origin are not yet understood, in most of the holocrystalline clasts. The abundance of granite clasts is particularly high for lunar brec-

cias, comprising up to 20% of the lithic clast population in some portions (though usually much less than this). Compston *et al.* (1975) assess the primary igneous age of the granites as 4.03 ± 0.03 b.y.

2.6. Ilmenite microgabbros

Apparently restricted to the Marble Cake clast of 72275, the ilmenite microgabroos (Figure 10d) are a fine-grained, KREEP-rich (Table II, cols. 10–11) holocrystalline rock-type not reported from other lunar samples. They contain 43–57% modal plagioclase ($An_{65-80}Or_{5-15}$, Figure 6); 25–46% pyroxene ($En_{30-34}Wo_{45}$ and En_{48-53} Wo_{6-8} in equal abundance, Figure 7); and 9–18% ilmenite, phosphates, and trace amounts of cristobalite, troilite, and metallic iron. The wide pyroxene solvus and the texture (Figure 10d) may represent either recrystallization or a plutonic origin involving slow cooling from an initial high temperature. Exsolved pyroxenes in the Marble Cake show a similar solvus, but have not been found within any lithic clasts.

2.7. Ultramafics

Small fragments consisting mainly of mafic minerals with granulitic textures are rare, but include harzburgite and lherzolite, which may be remnants of ultramafic rocks rather than mafic-rich fragments of plagioclase source-rocks. However no systematic survey has been made.

2.8. Glassy clasts

Glasses in general are rare in Boulder 1 (with the exception of the granite clasts), but small undevitrified glassy fragments occur in samples 72215, 72235, and 72275. Sparse devitrified brown glass clasts also occur in 72275. Most of these are glassy-matrix breccias; pure glass fragments are rare. The few that have been analyzed have the composition of anorthositic gabbro.

2.9. Devitrified maskelynite

Devitrified glasses, interpreted as maskelynite, form a volumetrically important group in all boulder samples. Although most are rather pure plagioclase, a few contain minor amounts of mafic minerals. Two main types have been recognized. The first is similar to the shocked plagioclase of the Civet Cat clast, and is fine-grained with a distinct equilibration rim. The second, more common, type consists of a variolitic mosaic of radiating fibrous plagioclase. No undevitrified glasses of plagioclase composition have been observed in the boulder.

2.10. Monomineralic fragments

Apart from the small fragments considered as matrix materials, monomineralic fragments occur in grain sizes greater than 200 μ. Only plagioclase, pyroxene, and olivine are abundant, and some are over 2 mm in dimension. They must be derived from coarse-grained rocks, some of which have not been seen as lithic fragments and whose character is unknown. No systematic analytical study of the large fragments has been

performed, but the data suggests that the ranges of compositions are similar to those of the smaller fragments. Exsolved pigeonites, texturally similar to those observed in the Station 6 boulder (Heiken *et al.*, 1973), are derived from coarse rock-types that have not been observed as lithic clasts. It is not known whether all these are from the same source or whether they have diverse origins. Some may be derived from coarse-grained equivalents of the ilmenite microgabbros, although such a conclusion is tenuous. The exsolution textures are those of unmixing through a slow temperature drop, and are not produced by shock. The source of rare (100 μ) zircons is also unknown.

2.11. Gray to black competent breccias (GCBx and BCBx)

Gray to black competent breccia is the dominant lithology of the collected samples, though not necessarily of the boulder. It occurs as abundant clasts and rims in the light matrix of sample 72275 (Figure 11a) and forms the matrices of the clast samples 72215, 72235, and 72255. Some GCBx and BCBx form rims around other competent breccia clasts and around other lithic clasts (Figure 11b). A breccia-within-breccia sequence is common, and there is a continuous size distribution of the clasts. GCBx and BCBx matrices have varying degrees of porosity (generally less than 10%) and there is a complete color gradation between clasts, from gray to black; most of the rim materials are very dark. Although many clasts have globular shapes, some are angular and broken. The competent breccias contain all of the previously described lithologies with the exception of the quartz-normative pigeonite basalts (PB).

The matrices of the GCBxs and BCBxs are dark and opaque or semi-opaque in transmitted light, although most are a lighter gray in macroscopic observation. Macroscopically the darker varieties have a vitreous luster, but matrix glass is extremely rare. The breccias are matrix-rich, consisting largely of densely welded fragments that are frequently less than 20 μ in diameter. The opacity is at least partly due to the presence of abundant finely-dispersed metallic iron. The fragment size distribution is continuous, and the matrix texture (Figure 11c) is generally similar to medium- and high-grade metamorphosed breccias described by Warner (1972). Small patches with a melt texture exist (below). Probe analyses show that some of the monomineralic olivines have equilibration rims 10 to 15 μ wide, though minerals in general have not equilibrated with the matrix to any substantial degree. The total lack of similar rims in the surrounding LFBx matrix suggests that the metamorphism affected the GCBx materials alone and not the boulder as a whole.

Any particular zones or domains of GCBx and BCBx seem to have a consistent bulk composition. Columns 12–13 of Table II are analyses of two different portions of 72215 Domain 5 (terminology of Stoeser *et al.*, 1974a); the only significant difference is in the P_2O_5. Different zones or clasts have different compositions, ranging from anorthositic norite to high-alumina basalt (classification of Prinz *et al.*, 1973), though most contain a KREEP component (Table II, cols. 14–17 and Blanchard *et al.* (1975)). Most are moderately KREEPy olivine-normative norites, whose compositions are common at the Apollo 17 site (Blanchard *et al.*, 1975).

Portions of the matrix have a texture which is clearly igneous rather than clastic, consisting of euhedral pyroxenes set in a matrix of plagioclase; patches of glassy mesostasis are present (Figure 11d). The texture is more prevalent in the KREEPier breccias, and the analyzed portions are of a very KREEP-rich basaltic composition (Table II, col. 18). However, the clearly igneous texture is uncommon, and it is impossible to be certain that more than a minor portion of the matrix crystallized from a melt. The larger patches of melt seem to be the result of partial melting of the breccia during metamorphism rather than impact melts: they contain no nickel measurable with the microprobe, and they have compositions similar to those to be expected from the partial melting of a KREEPy breccia. If they are impact melts the

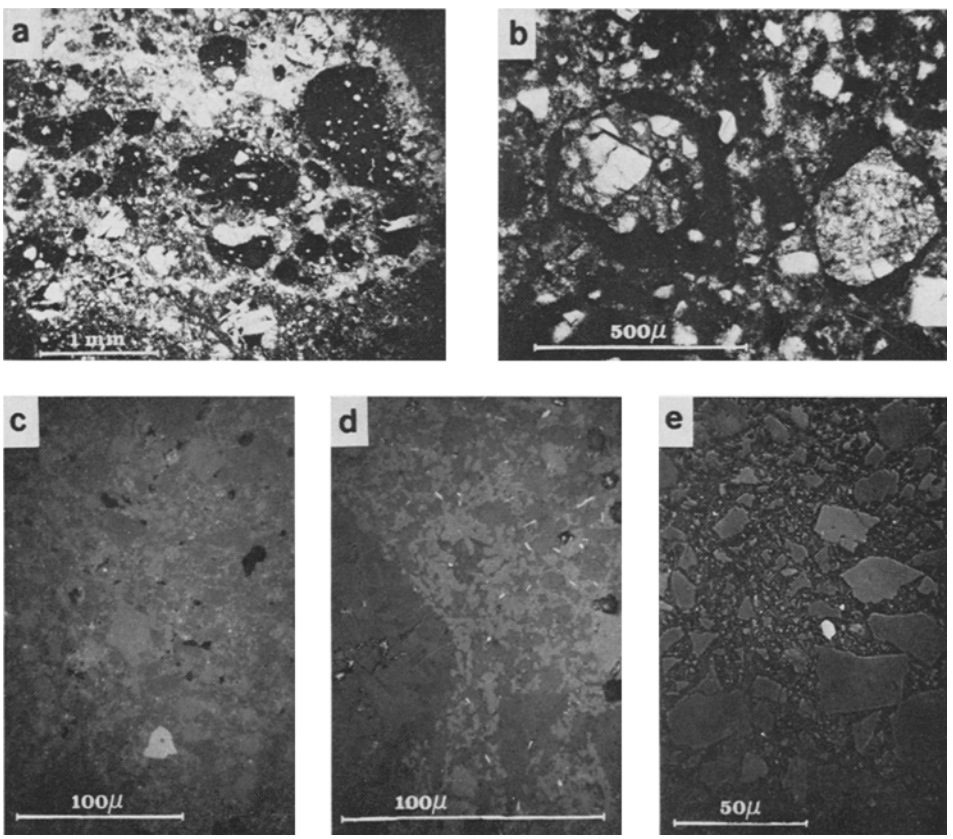

Fig. 11. Photomicrographs of boulder breccias: (a) GCBx clasts in 72275 LFBx; note also PB fragment. Plane polarised light. (b) BCBx-rimmed anorthositic breccia and granulitic ANT clasts in 72275. Plane polarised light. (c) Typical GCBx clastic matrix in 72255, mainly consisting of plagioclase (dark gray) and pyroxene (medium gray). Also visible are a spinel grain (lower middle, light gray) and tiny ilmenite grains. Reflected light. (d) Partially molten portion of GCBx material in 72215, with euhedral pyroxenes (medium gray) set in plagioclase groundmass (dark gray). Glassy mesostasis (very dark gray) is visible. The clast at the left-hand side is a holocrystalline granite fragment which appears to be partially melting along grain boundaries. Reflected light. (e) Matrix of 72275 LFBx, showing porosity and friable nature, in contrast to the GCBx matrices.

composition of the target rock was unlike any observed clast-type within the boulder. It is possible that some of the material binding the competent breccias together is an impact melt, as has been suggested by James *et al.* (1975) for 73215. However, these melts must be minor in abundance, and their compositions are not obviously dissimilar to the breccias as a whole. Thus the melt patches, whatever their origin, do not explain the KREEPy nature of the breccias.

Stoeser *et al.* (1974a) and Blanchard *et al.* (1974) have assumed that the compositions of the GCBxs and BCBxs are the result of the intimate mixing of the clast-types present within them. However most of the clast-types observed are more aluminous than the competent breccia matrices, and production of the GCBxs and BCBxs requires the mixture of a less aluminous and more iron-rich and KREEPy component with the observed clast-types (Figures 2–4).This component is not the PB, as has been previously proposed (Stoeser *et al.*, 1974a; Blanchard *et al.*, 1974). The PB has an unusually high and distinctive germanium content (Morgan *et al.*, 1975), which would

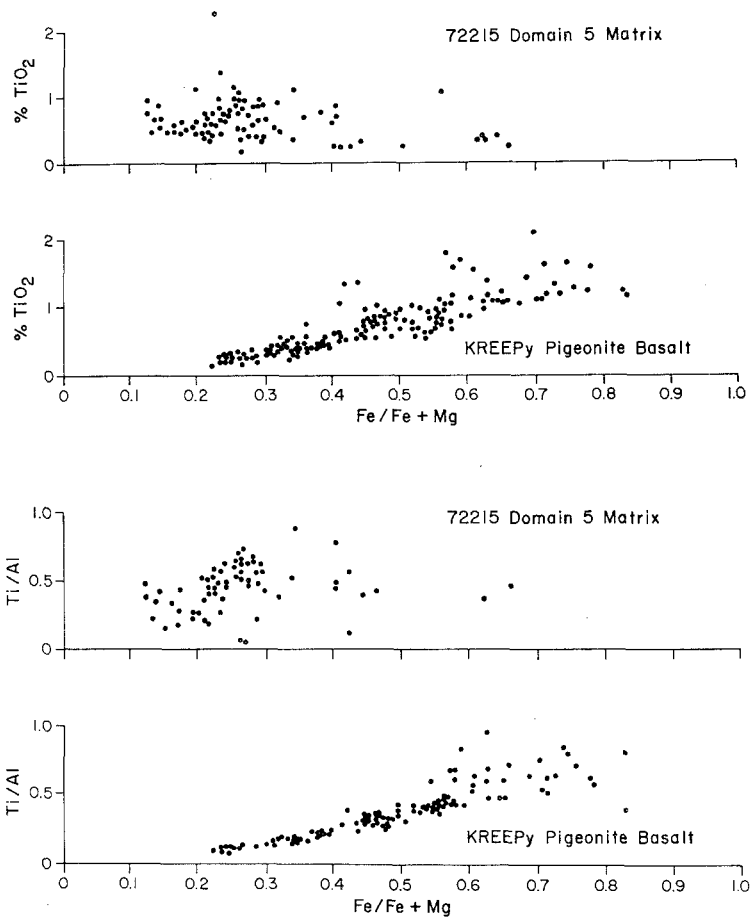

Fig. 12. Comparison of pyroxenes in the 72215 Domain 5 (GCBx) matrix with those in KREEPy pigeonite basalt (PB); top, TiO_2 v. Fe/Fe+Mg; bottom, Ti/Al v. Fe/Fe+Mg.

be reflected in the competent breccias if the PB was abundant enough to satisfy the major element requirements; the competent breccias do not have the necessary germanium abundances (Morgan *et al.*, 1975). Also, very few pyroxene fragments in the breccia, at least those larger than 10 μ, are identical in composition to those found in the PB clasts if Ti, Al, and Cr are considered as well as the major elements. Figure 12 shows Ti and Al compositions for pyroxenes from the PB and from the matrix of 72215 Domain 5 (a KREEP-rich breccia which can reasonably be stated to contain more of the KREEP-rich unknown component than other breccias). PB pyroxene compositions are conspicuously rare; in the apparent overlap regions in Figure 12 the matrix pyroxenes are calcium-poor compared to those in the PBs. Finally, no PB clasts have been observed in the GCBxs and BCBxs. Therefore if the component is

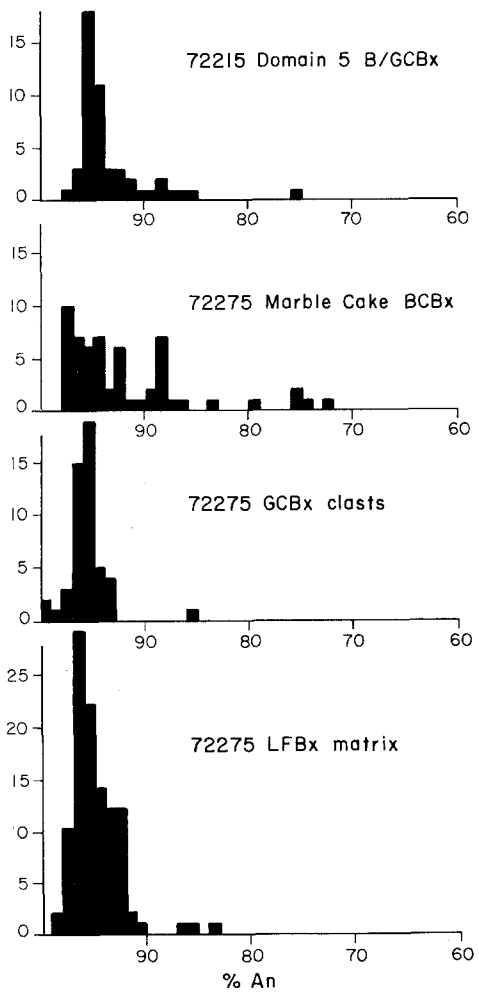

Fig. 13. Plagioclase compositions for some boulder competent breccia matrices and light friable matrix, shown as histograms rather than on ternary diagrams to demonstrate the predominance of high-Ca varieties.

PB it is so extremely finely comminuted that not even pyroxene fragments survive. This seems unlikely, and combined with the germanium evidence, is strong evidence that the PB is not the unidentified cryptic component.

The KREEPy nature of the matrices could be provided by the *K*-ANT or by the granites. The percentage of granite clasts within any competent breccia does show a broad correspondence with the *K*-content of the matrix (from data in Stoeser *et al.*, 1974a). However neither the *K*-ANT nor the granite provides the major-element mass-balance required, and therefore at least one other unidentified component is present in the matrix. We will return to this question of the unidentified component below.

The matrix consists of ubiquitous plagioclase, pyroxene, and olivine, and ilmenite, phosphates, and Fe-metal. More scattered components are silica, *K*-feldspar, ternary feldspar, pink spinel, troilite, chromite, and rare zircon. The proportions, particularly of olivine and phosphate, are variable, and correspond to the variability of the bulk chemistry. Presumably the mineralogy provides clues to the nature of the source-rocks from which the matrix was derived. Microprobe analyses of numerous matrix grains (mainly those larger than 20 μ) have been made in an attempt to define lithic clast-types in the source-region.

Plagioclase compositions (Figure 13) are indistinctive and correspond to typical lunar fields and to plagioclase in many of the clast-types in the boulder. The distributions peak at around An_{94} or An_{95}, but a more varied pattern exists for the Marble Cake rind. The olivines (Figure 14) span a compositional range similar to those of the ANT and troctolitic rocks, but some iron-rich olivines ($\sim Fo_{50}$) may be derived from olivine-normative pigeonite basalts. Both the olivines and pyroxenes have ranges of

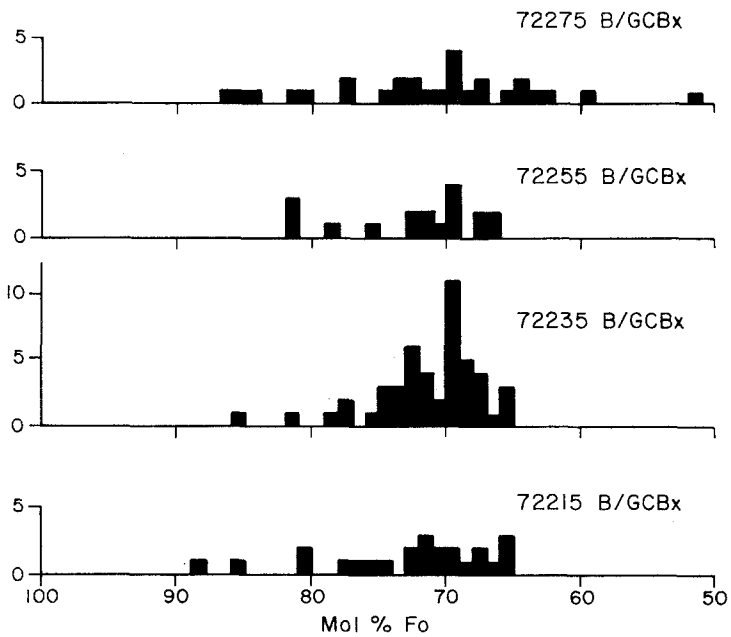

Fig. 14. Histograms of olivine compositions for some boulder competent breccia matrices.

compositions which differ between individual breccia zones (Figures 14 and 15), indicating that the different competent breccias have different source lithologies. Most, but not all, of the pyroxenes (Figure 15) are low-calcium varieties equivalent to those in the lithic clast-types; augitic pyroxenes equivalent to those in lithic clasts are also

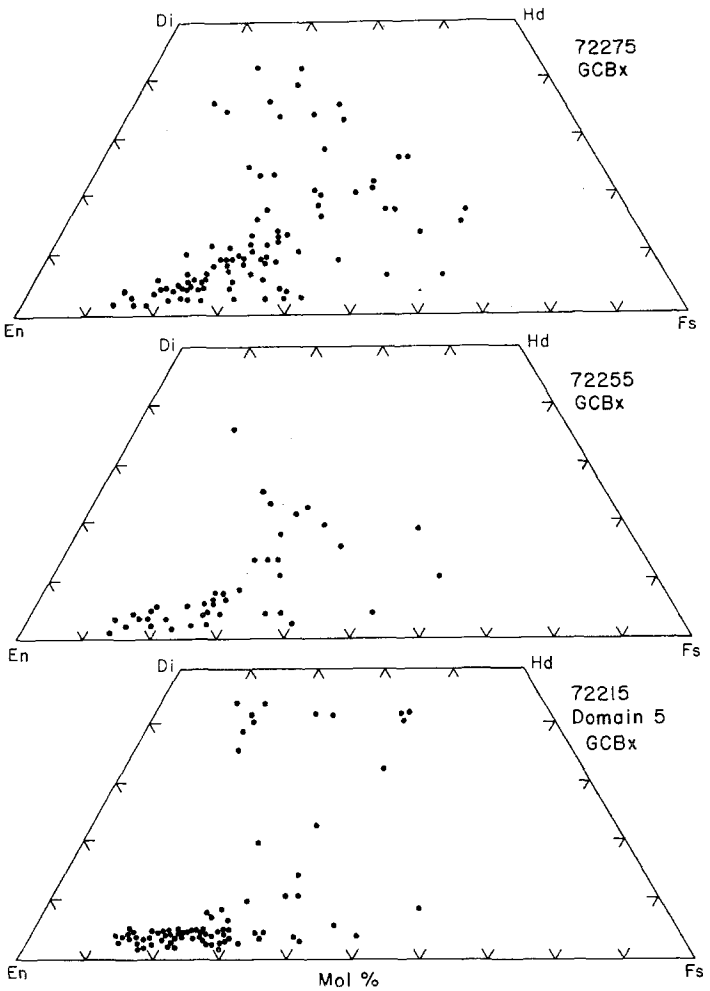

Fig. 15. Plots of pyroxene compositions for some boulder competent breccia matrices.

present. Some pigeonitic pyroxenes do not have equivalents within lithic clasts and may thus characterize the unknown component or components; this component may therefore have been basaltic. Pyroxenes chemically and texturally similar to those in the Civet Cat clast are ubiquitous in the competent breccias. There is more ilmenite in the competent breccias than can reasonably be derived from observed clasts, and some ilmenite may be derived from the unknown component. Similar arguments apply to phosphorous, though some of this can be derived from *K*-ANTs,

KREEP-norites, or the parent rock of the granite clasts. Silica fragments, *K*-feldspar, and ternary feldspars are most easily attributed to the granites, since abundant granite clasts occur in the matrix. The pink spinels present a problem, for they are frequently too large to be derived from the pink-spinel troctolitic basalts, which in any case are not an abundant clast-type. The parent of the spinels has therefore not been observed and represents still one more unidentified, if minor, component.

In summary, the GCBxs and BCBxs are composed of welded fragmental debris, some of which is correlatable with lithic clast-types contained within the boulder and some of which is not. The main unidentified component is apparently of a KREEP-rich basaltic composition which exists in the matrix and either did not exist or failed to survive as lithic clasts during the assembly of the GCBxs and BCBxs. This suggests that it was fine-grained during assembly of the competent breccias, either in a clastic

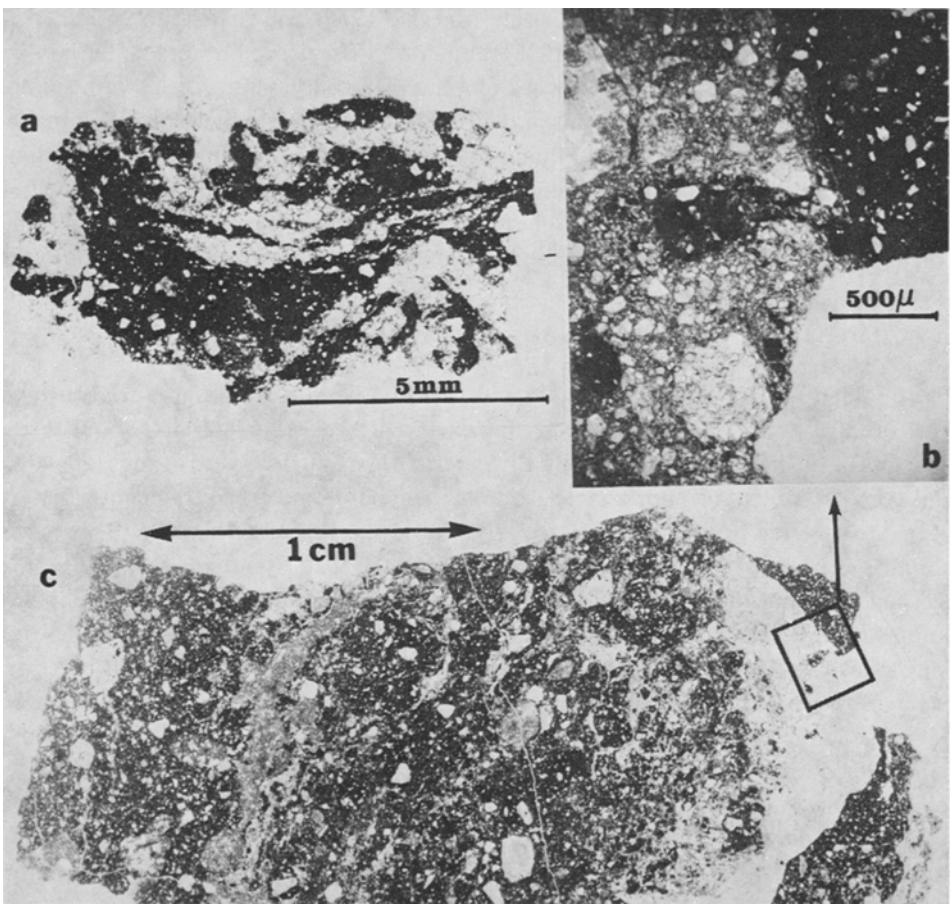

Fig. 16. (a) Thin section 72275, 140, Marble Cake rim, showing lamination and 'stirring'. Plane polarised light. (b) Dying Dog (72235) rim material, showing injection of GCBx material (black) into crushed granulitic anorthositic norite. Plane-polarised light. (c) Thin section 72235,59, from which (b) is taken; note stirring of core and rim. Plane-polarised light.

or in a melt form. A discussion of the genesis of the GCBxs and BCBxs is deferred until other relevant aspects have been considered.

2.12. Marble cake clast (clast # 1), 72275

Macroscopic examination suggested that this 3-cm clast was a cataclastic gabbroic anorthosite crudely interlayered with gray breccia and dark rim material. Thin sections showed that the rim and the core have been fluidized and interlayered in a rather complex manner to form a 'marble cake' pattern (Figure 16a). The dark rim is a black competent breccia that is more vesicular than most. The white core clasts include anorthositic norites of various textures and the unique ilmenite microgabbros, as well as granites and other small lithic fragments (Marvin *et al.*, 1974).

2.13. Dying dog clast (72235)

72235 consists of the Dying Dog clast (Marvin, 1975) and a portion of adhering LFBx which is similar to that of 72275, though no PB has been observed. Serial thin sections show that the clast is composed of a number of different breccias with a complex structural history. The materials of the rind BCBx and the lighter-colored anorthositic layers have been crushed and fluidized during or after their mutual aggregation; thin veinlets of the rind material penetrate the interior along minute cracks (Figures 16b, c); conversely, veinlets of the light material penetrate the rind. Thus the rims and cores were mobile at the same time, and the rim is not merely an aggregation onto the core.

3. Light-Gray Friable Matrix (LFBx)

The boulder matrix, sampled in 72275 and part of 72235, is a light-gray friable polymict breccia, consisting of about 60% matrix and 40% clastic materials; about three-quarters of the latter is GCBx and BCBx material. The matrix is very porous (20–40%) and consists largely of poorly sintered angular mineral and lithic fragments (Figure 11e). Most of the lithic fragments are ANT varieties. Pigeonite basalt (PB) breccias occur as clots and bands up to 2 cm thick within the matrix and are essentially pure crushed pigeonite basalt clasts. Civet Cat norite and granites, common within the competent breccias, appear to be absent from the LFBx. Neither glass spherules nor ropy glass clasts, nor their devitrified equivalents characteristic of regolith breccias, occur in the light matrix. The range of mineral fragment compositions is similar to the range in the GCBxs, with plagioclase, low-calcium pyroxene, and olivine predominant. Ilmenite, troilite, Fe-metal, pink-spinel, chromite, and trace amounts of *K*-feldspar, silica, zircon, and armalcolite are present.

Although the bulk composition of the matrix (PET, 1972; Blanchard *et al.*, 1975; Stoeser *et al.*, 1974b) is broadly similar to that of the GCBxs, the trace element analyses indicate that it is not identical, at least for the particular materials analyzed. For instance, it contains only half of the meteoritic abundances of the GCBx matrix of 72255 and also has higher germanium contents, in part a reflection of the pigeonite basalt clasts (Morgan *et al.*, 1975). These characteristics, combined with the total lack

of pigeonite basalt clasts in the GCBxs, preclude the possibility of the LFBx being merely a crushed version of the GCBx as suggested by Stoeser *et al.* (1974a). The lack of equilibration rims and the lack of extensive sintering suggest that the matrix was not subjected to high temperatures for any great length of time.

4. The History of the Boulder Materials

Figure 1 illustrates the general relationships of the boulder constituents, as deduced from simple geological principles. The oldest clasts are those contained in the competent breccias (GCBxs) and include ANT clasts, troctolitic basalts, granitic fragments, and the Civet Cat clast. The GCBxs and BCBxs are complex, with rims of competent breccia material surrounding clasts of other competent breccia material, and competent breccia clasts lying in a competent breccia matrix. The competent breccias lie in a matrix of the light friable matrix, which is apparently a distinct textural and chemical entity; it also contains pigeonite basalt clasts that are not found within the competent breccia matrices. We cannot assume that the unrimmed ANT clasts and other lithic clasts found in the LFBxs are derived from the identical source-region as those rimmed or enclosed by the GCBxs or BCBxs, though it is possible.

The important questions which the simple sequence leaves unanswered are those concerning the origins of the lithic clasts, especially the origin of the GCBx and BCBx clasts, and the relationship of the latter breccias to the LFBx matrix. These questions require evidence additional to the stratigraphic considerations.

4.1. The genesis of the BCBxs and GCBxs

The GCBxs consist of an agglomeration of clastic materials, including earlier GCBx and BCBx clasts which were later fluidized, stirred, and welded. Some of the clastic material of the matrix can be derived from the comminution of recognizable lithic clast-types, but the matrix contains a component of KREEP chemistry that is not observed as a lithic clast-type (above). The nature and source of this material is obscure. If the breccia had a single-stage history of comminution of the lithic clast-types from which it is built, then it is likely that the unknown component, if it was a holocrystalline variety, would have survived in the form of at least a few clasts. That it did not suggests that this component was already a fine-grained material prior to the GCBx formation. This leads in turn to the conclusion that the GCBxs consist in large part of preexisting breccia material that probably experienced more than one brecciation event. This is not unlikely considering the amount of material that must exist in ejecta blankets which are potential target areas for impacts. 14321, for instance, also contains breccia-within-breccia sequences (Grieve *et al.*, 1975; personal observation by Ryder). The breccia-within-breccia sequence in Boulder 1, and the clasts enclosed by rims of competent breccia further enclosed in a competent breccia matrix, are obviously complicated agglomerational features; the relationships in the complex rimmed clasts additionally demonstrate a complicated post-aggregational history of stirring and crushing prior to sintering of the constituent grains.

The formation of the GCBxs involved an intense thermal event. Sintering experiments (Hallam, 1974) suggest temperatures in excess of 900 °C for dry sintering of GCBx materials, and at least several days would be required to produce the magnitude of sintering observed in the GCBx samples. The presence of partial-melting products of the breccias themselves also suggests high and prolonged temperatures; in the system An–Fo–Si with Fe/Fe+Mg ~0.3 (Walker *et al.*, 1973), which is appropriate here, the temperature of first melting is about 1150 °C. The absence of undevitrified maskelynite indicates annealing temperatures of 800 °C or more for several hours (Anderson *et al.*, 1972). Finally, the presence of granitic glasses at the time of breccia formation indicates temperatures in excess of 990 °C (Levin *et al.*, 1964). We conclude that the GCBx materials are the result of extensive metamorphism involving partial melting of materials which consisted of lithic clasts and debris from multi-processed breccia materials. However, it should be pointed out that this conclusion may be in conflict with the Sr isotope data, which suggests that the thermal event was 'short-lived' (Compston *et al.*, 1975,) and that it is not held by all Consortium members (cf. Wood, 1975).

4.2. Genesis of the light matrix breccia and its relationship to the competent breccia materials

The relationship of the competent materials to the friable materials is of paramount importance in assessing the constructional history of the boulder. It has previously been proposed that the GCBx was formed by sintering of the LFBx (Stoeser *et al.*, 1974b; Hallam, 1974) and that the LFBx was formed by the shearing of the GCBx materials. However it is probable that no direct relationship exists between the two lithologies for the reasons given above: i.e. they are not chemically identical, nor do their clast populations coincide. If the LFBx were a variety of GCBx, pigeonite basalt should be present in the latter; it has not been observed.

If the friable nature of the LFBx was produced by the shearing that is evident in the boulder, it is likely that the GCBxs would have been affected. That this does not seem to be the case suggests that the friable matrix was always more friable: it was affected by shearing simply because it was so poorly consolidated at the time that the shearing event took place. This suggests in turn that the LFBx was created in a cooler and distinct environment, and from a different source-material than the GCBx, though it is possible that this was merely a later stage of the same overall event (Wood, 1975). If Wood's model is correct, the formation of the GCBxs would have taken place in a growing hot transient cavity rather than in an ejecta blanket. However, the GCBx clasts have sharp boundaries with the LFBx as seen in photographs and in reflected light under the microscope, despite Schmitt's (1976) observation that the boundaries are gradational. The lack of any evidence in thin sections for contact metamorphism suggests that at least the smaller GCBx clasts were cool during their incorporation into the LFBx. The magnetic evidence (Banerjee and Swits, 1975) suggests that even the large GCBx clasts (whose contacts have not been observed under the microscope) had already cooled far below the temperature of their partial melting at the time they

were incorporated into the LFBx. Therefore the GCBx could not have formed in an early stage of the same event that produced the LFBx matrix; such an event would have a time-scale of minutes, rather than the hours required to partially melt and cool the GCBxs before the assembly of Boulder 1, Station 2. This interpretation views the 'globby' shape of some of the GCBx clasts as an abrasional feature rather than as the semi-hydrostatic response of a small plastic body; the rims on lithic clasts are seen as the remnants of a more extensive GCBx matrix that previously enclosed the clasts. We therefore favor separate events for the genesis of the two breccias, with the LFBx forming in a much cooler environment. This does not necessarily mean that the LFBx-producing impact event was less intense than the GCBx-forming event, because a single event would produce a wide variety of depositional environments.

The apparently unique occurrence of the PB in Boulder 1, Station 2 remains a disturbing question. Is the PB a very rare rock-type, sampled only by chance in Boulder 1, or is Boulder 1 exotic to the Taurus-Littrow site?

4.3. The relative boulder history

Based on the above arguments, our interpretation of the major events in the relative boulder history can be summarized as follows:

(1) An obscure early history of production of lithic clast-types, involving magmatism, brecciation, and metamorphism, producing a lithic clast-bearing breccia terrain.

(2) An impact, sufficient to melt granite and create a hot ejecta blanket, in which breccias and lithic clasts were agglomerated, mobilized, and metamorphosed (formation of the GCBx and BCBx).

(3) Extrusion of the PB onto the lunar surface near or onto the ejecta blanket produced in (2).

(4) An impact, creating a cool ejecta blanket, insufficient to sinter the new matrix. The source terrain included the ejecta blanket created in (2), the PB, and possibly a freshly exposed ANT-like highland terrain. This event may have emplaced the boulder materials in the South Massif.

(5) Shearing of the boulder matrix, possibly as a late stage of (4).

(6) Excavation of the boulder and emplacement at Station 2, Apollo 17.

Isotopic age determination on boulder samples provide constraints on the absolute ages of these relative events. A further constraint is provided by the onset of mare volcanism in the Taurus-Littrow region, because the boulder is believed to be a South Massif deposit (AFGIT, 1973) and contains no mare basalt fragments. Therefore, its formation pre-dates mare activity – i.e. it is pre- $\sim$3.8 b.y.

^{39}Ar–^{40}Ar determinations give a plateau age for the 72255 GCBx matrix of 4.01 $\pm$ $\pm$0.03 b.y. (Leich *et al.*, 1974), which dates event (2) in our sequence. This age is supported by the Rb/Sr isochron ages (Compston *et al.*, 1975) of the Civet Cat clast and of the granite clasts, which are older than this age. The extrusion age of the PB is 4.01 $\pm$ 0.04 b.y. (Compston *et al.*, 1975) and is thus of a similar age to the GCBx. The formation of the LFBx is later than this, but it is not as young as the mare basalts; unfortunately the ^{39}Ar–^{40}Ar plateau ages are not meaningful (Leich *et al.*, 1974).

The petrographic relationships and the age data thus demonstrate a complex and prolonged history for the boulder samples, extending back to at least 4.17 b.y. (Civet Cat clast, Compston *et al.*, 1975). After this time, and possibly around 4.01 b.y., an impact occurred, creating a hot ejecta blanket in which the competent breccias were formed. This impact was probably quite large, possibly of basin-forming magnitude. PB was extruded onto the lunar surface very shortly afterwards, or maybe penecontemporaneously. A later impact created a new, cooler ejecta blanket, in which the light friable boulder matrix was formed. At a still later date mare basalt extrusion commenced.

At present the boulder-forming events cannot be assigned with certainty to specific impacts, and several possibilities exist. The Taurus-Littrow region lies on the edge of the Serenitatis basin, and the impact responsible for this basin created the South Massif. Within the framework of the relative boulder history outlined above, the main possbilities are:

(a) The boulder is wholly pre-Serenitatis, and is a clast within the Serenitatis ejecta blanket. This would date the Serenitatis event as younger than 4.01 b.y.

(b) The boulder LFBx is Serenitatis ejecta, and the GCBx clasts are pre-Serenitatis. In this model the Serenitatis event is also younger than 4.01 b.y.

(c) The GCBx is Serenitatis ejecta, which would therefore be dated at 4.01 b.y.; the LFBx is a later deposit that merely formed a mantle on the South Massif.

(d) Both LFBx and GCBx/BCBx are post-Serenitatis, which was therefore pre-4.01 b.y.

Although a definitive assignment cannot be given, the latter two possibilities seem the least likely because the blue-gray breccia from which the boulder is believed to be derived (Schmitt, 1973) forms a considerable thickness on the South Massif. This implies that it must have been deposited in the Serenitatis event rather than in a later event such as Imbrium (Wolfe and Reed, 1974).

Meteoritic elements suggest that the whole boulder is different to other Taurus-Littrow highlands breccias, which are presumably mainly Serenitatis ejecta, and the boulder may therefore not be Serenitatis ejecta. Wolfe and Reed (1974) have suggested on stratigraphic grounds that the boulder was a large clast within the Serenitatis ejecta blanket. Although petrographically it is tempting to consider the whole boulder as pre-Serenitatis because of its distinct clast population, the boulder matrix is very friable and Boulder 1 as a whole probably could not have withstood rapid movement over substantial distances without breaking up. It has also been observed (Warner, 1972) that at the scale of the hand-sample, clasts are of a grade of metamorphism higher than or equivalent to their host breccias. If this relationship is also true for the ejecta blanket scale, then the LFBx is unlikely to be a clast in a hot ejecta blanket that may best be represented for the Apollo 17 site by the boulders at Station 6. The evidence for the relationship of Boulder 1 to the Serenitatis event is therefore conflicting.

We suggest that the LFBx was created in the Serenitatis event, in a cool upper portion of the ejecta blanket (model (b), above) and that the GCBx clasts were created

in an earlier impact event. This implies that the Serenitatis event is younger than 4.01 b.y. Many breccias from the Apollo 17 highlands have ages in the 3.95–4.00 b.y. range (Husain and Schaeffer, 1975), compatible with a Serenitatis event at this time. (Husain and Schaeffer, however, allocated these ages to the Imbrium event and dated the Serenitatis event at 4.26 b.y. on the age of one other rock.)

5. The Lunar Crust Before Boulder Formation

The boulder clast population demonstrates a complex and varied history of magmatism, metamorphism, and brecciation in the lunar crust in the interval between the origin of the Moon (~4.6 b.y.) and the assembly of the boulder (later than or equal to 4.01 b.y.). Magmatism is demonstrated by the granites, which are presumably a plutonic differentiate, possibly related to the KREEP-norite and ilmenite microgabbros in a larger layered intrusion. The Civet Cat norite probably attests to yet another and earlier magmatic phase, and many of the ANT clasts were ultimately probably of igneous origin, possibly including remnants of the primordial lunar differentiation. A late event was the extrusion of a KREEPy basalt whose composition may indicate greater degrees of partial melting of a source-region similar in some respects to that which produced the Apollo 15 KREEP basalts. Some or all of the pink spinel troctolitic basalts, olivine basalts, and troctolitic basalts may also represent partial melting products of the lunar interior.

In any case, the Moon was not a thermally passive body between the primordial differentiation and the commencement of mare basalt extrusion, but may have been continually heated in its interior, causing metamorphism and partial melting. At the same time, the continued bombardment of the lunar crust disrupted the products of the magmatic activity, creating breccias and probably creating impact melts. Many of the materials represent several generations of events, and the boulder is thus a palimpsest from which earlier events have not been fully read, and from which the earliest events may have been completely erased.

6. Conclusions

The boulder consists of two separate entities: an older metamorphosed breccia containing a diverse lithic clast population, and a friable matrix containing KREEPy basalts. The light-gray friable matrix was probably deposited in a cool upper portion of the Serenitatis ejecta blanket in the South Massif sometime after 4.01 b.y. An older, hotter ejecta blanket was responsible for the metamorphism of the competent breccias that are now clasts within the friable matrix. The source terrain for this earlier ejecta blanket contained granite and lithologies not observed elsewhere in lunar samples. The presence of these unfamiliar lithologies and the KREEPy basalts in the friable matrix emphasize that the boulder is a unique lunar sample, providing information concerning the evolution of the Moon between its formation and the time of breccia assembly.

Acknowledgements

We wish to thank Karen Motylewski for editing and typing the manuscript. This research has been supported by NASA Grant NGL 09-105-150.

References

AFGIT (Apollo Field Geology Investigation Team): 1973, *Science* **182**, 672–680.
Anderson, A. T., Brazunas, T. F., Jacoby, J., and Smith, J. V.: 1972, *Proc. Third Lunar Sci. Conf.* **1**, 819–835.
Banerjee, S. K. and Swits, G.: 1975, this issue, p. 473.
Bence, A. E., Papike, J. J., Sueno, S. S., and Delano, J. W.: 1973, *Proc. Fourth Lunar Sci. Conf.* **1**, 597–611.
Blanchard, D. P., Haskin, L. A., Jacobs, J. W., Brannon, J. C., and Korotev, R. L.: 1974, *Interdisciplinary Studies of Samples from Boulder 1, Station 2, Apollo 17*, L.S.I. Contr. No. 211D, pp. IV-1–IV-12.
Blanchard, D. P., Haskin, L. A., Jacobs, J. W., Brannon, J. C., and Korotev, R. L.: 1975, this issue p. 359.
Compston, W., Foster, J. J., and Gray, C. M.: 1975, this issue, p. 445.
Grieve, R. A., McKay, G. A., Smith, H. D., and Weill, D. F.: 1975, *Geochim. Cosmochim. Acta* **39**, 229–245.
Hallam, M. E.: 1974, *Interdisciplinary Studies of Samples from Boulder 1, Station 2, Apollo 17*, L.S.I. Contr. No. 210D, pp. 111–120.
Heiken, G. H., Butler, P., Phinney, W. C., Warner, J., Schmitt, H. H., Bogard, D. D., Simonds, C. H., and Pearce, W. G.: 1973, *NASA Tech. Mem. X-58116*, 56 pp.
Husain, L. and Schaeffer, O. A.: 1975, *Geophys. Res. Letters* **2**, 29–32.
James, O. B., Marti, K., Braddy, D., Hutcheon, I. D., Brecher, A., Silver, L. T., Blanchard, D. P., Jacobs, J. W., Brannon, J. C., Korotev, R. L., and Haskin, L. A.: 1975, *Lunar Science VI*, The Lunar Science Institute, pp. 435–437.
Leich, D. A., Kahl, S. B., Kirschbaum, A. R., Niemeyer, S., and Phinney, D.: 1974, *Interdisciplinary Studies of Samples from Boulder 1, Station 2, Apollo 17*, L.S.I. Contr. No. 211D, pp. VI-1–VI-18.
Levin, E. M., Robbins, C. R., and McMurdie, H. F.: 1964, *Phase Diagrams for Ceramists*, Am. Ceramic Soc., Columbus, Ohio, p. 158.
Marvin, U. B.: 1974, *Interdisciplinary Studies of Samples from Boulder 1, Station 2, Apollo 17*, L.S.I. Contr. No. 210D, pp. 9–33.
Marvin, U. B.: 1975, this issue, p. 315.
Marvin, U. B., Stoeser, D. B., and Bower, J. F.: 1974, *Meteoritics* **9**, 377–379.
McCallum, I. S., Mathez, E. Z., Okamura, F. P., and Ghose, S.: 1975, *Lunar Science VI*, The Lunar Science Institute, pp. 534–536.
Morgan, J. W., Higuchi, H., and Anders, E.: 1975, this issue, p. 373.
PET (Apollo 17 Preliminary Examination Team): 1973, *Science* **182**, 659–672.
Prinz, M., Dowty, E., Keil, K., and Bunch, T. E.: 1973, *Geochim. Cosmochim. Acta* **37**, 979–1006.
Ryder, G., Stoeser, D. B., Marvin, U. B., and Bower, J. F.: 1975, *Proc. Sixth Lunar Sci. Conf.*, in press.
Schmitt, H. H.: 1973, *Science* **182**, 681–690.
Schmitt, H. H.: 1975, this issue, p. 491.
Simonds, C. H., Warner, J. L., and Phinney, W. C.: 1973, *Proc. Fourth Lunar Sci. Conf.* **1**, 613–632.
Stoeser, D. B., Marvin, U. B., and Bower, J. F.: 1974a, *Interdisciplinary Studies of Samples from Boulder 1, Station 2, Apollo 17*, L.S.I. Contr. No. 211D, pp. III-1–III-51.
Stoeser, D. B., Wolfe, R. W., Wood, J. A., and Bower, J. F.: 1974b, *Interdisciplinary Studies of Samples from Boulder 1, Station 2, Apollo 17*, L.S.I. Contr. No. 210D, pp. 35–109.
Stoeser, D. B., Marvin, U. B., Wood, J. A., Wolfe, R. W., and Bower, J. F.: 1974c, *Proc. Fifth Lunar Sci. Conf.* **1**, 355–377.
Taylor, G. J., Marvin, U. B., Reid, J. B., Jr., and Wood, J. A.: 1972, *Proc. Third Lunar Sci. Conf.* **1**, 995–1014.

Walker, D., Grove, T. L., Longhi, J., Stolper, E. M., and Hays, J. F.: 1973, *Earth Planetary Sci. Letters* **20**, 235–236.
Warner, J. L.: 1972, *Proc. Third Lunar Sci. Conf.* **1**, 623–643.
Wilshire, H. G. and Jackson, E. D.: 1972, *Earth Planetary Sci. Letters* **16**, 396–400.
Wolfe, E. W. and Reed, V. S.: 1974, *Interdisciplinary Studies of Samples from Boulder 1, Station 2, Apollo 17*, L.S.I. Contr. No. 211D, pp. I-1–I-19.
Wood, J. A.: 1975, this issue, p. 505.
Wood, J. A., Marvin, U. B., Reid, J. B., Jr., Taylor, G. J., Bower, J. F., Powell, B. N., and Dickey, J. S., Jr.: 1971, *SAO Special Rept. 333*, 272 pp.